Archives of Biochemistry and Biophysics 506 (2011) 99–108

Contents lists available at ScienceDirect

Archives of Biochemistry and Biophysics

journal homepage: www.elsevier.com/locate/yabbi

C-terminal fragment of amebin promotes actin filament bundling, inhibits acto-myosin ATPase activity and is essential for amoeba migration

Jolanta Jóźwiak [a], Yuriy Rzhepetskyy [b], Magdalena Sobczak [a], Elżbieta Kocik [a], Radosław Skórzewski [c], Wanda Kłopocka [a], Maria Jolanta Rędowicz [a,*]

[a] Nencki Institute of Experimental Biology, Warsaw, Poland
[b] Institute of Cell Biology, 14/16 Drahomanova St., 79005 Lviv, Ukraine
[c] Department of Biochemistry and Cell Biology, Kazimierz Wielki University, 30 Chodkiewicza St., 85-064 Bydgoszcz, Poland

ARTICLE INFO

Article history:
Received 6 August 2010
and in revised form 11 November 2010
Available online 19 November 2010

Keywords:
Actin
Actin cytoskeleton
Acto-myosin ATPase activity
Amebin
Amoeba proteus
Caldesmon
Crosslinking

ABSTRACT

Amebin [formerly termed as ApABP-FI; Sobczak et al. (2007) Biochem. Cell Biol. 85] is encoded in *Amoeba proteus* by two transcripts, 2672-nt and 1125-nt. A product of the shorter transcript (termed as C-amebin), comprising C-terminal 375 amino-acid-residue fragment of amebin, has been expressed and purified as the recombinant GST-fusion protein. GST-C-amebin bound both to monomeric and filamentous actin. The binding was Ca^{2+}-independent and promoted filament bundling, as revealed with the transmission electron microscopy. GST-C-amebin significantly decreased MgATPase activity of rabbit skeletal muscle acto-S1. Removal with endoproteinase ArgC of a positively charged C-terminal region of GST-amebin containing KLASMWEQ sequence abolished actin-binding and bundling as well as the ATPase-inhibitory effect of C-amebin, indicating that this protein region was involved in the interaction with actin. Microinjection of amoebae with antibody against C-terminus of amebin significantly affected amoebae morphology, disturbed cell polarization and transport of cytoplasmic granules as well as blocked migration. These data indicate that amebin may be one of key regulators of the actin-cytoskeleton dynamics and actin-dependent motility in *A. proteus*.

Introduction

Dynamic reorganization of actin cytoskeleton in response to various stimuli plays a key role in functioning of eukaryotic cells and is indispensable of the vital cellular processes such as migration, intracellular trafficking of particles and organelles, phagocytosis and cytokinesis. In cells, actin exists in two major pools, monomeric and filamentous ones, and a panoply of actin-binding proteins is responsible for precise controlling the state of actin polymerization/depolymerization and/or filament organization. This spatio-temporal regulation is possible due to the presence of specific domains/regions within these proteins, interacting with either actin monomers or filaments.

Actin filaments (microfilaments) can be organized *in vivo* into a number of defined structures such as filopodia, lamellipodia or stress fibers (see [1,2]). Dense actin filament network in lamellipodia is kept by protein cross-linkers such as filamin, spectrin or transgelin. Anchoring filaments to membranes and/or membrane proteins is possible due to the presence of α-actinin, tensin, talin or dystrophin. Filopodia formation, in which actin filaments are aligned into parallel linear arrays, is dependent on fascin, α-actinin and formins, and stress fibers can be formed due to the presence of not only fascin and α-actinin but also of conventional myosins II. There are also proteins such as nebulin, caldesmon or tropomyosin that act as the rulers and/or the filament stabilizers (see [2]).

Amoeba proteus, an unicellular organism, which length may reach up to 700 μm, has been widely used as a model to study motility of the crawling cells. Data gathered so far indicate that during interphase all amoeba motile processes depend only on dynamics of actin-based cytoskeleton [3]. Majority of amoeba filamentous actin is present in the perinuclear region and under plasma membrane cortex (ectoplasm), where it is organized into dynamic structures such as bundles and meshwork [4]. To date, only about a dozen of actin-binding or actin cytoskeleton-regulating proteins have been detected in these cells, including immunoanalogs of caldesmon [5], spectrin [6], α-actinin and vinculin [7], myosin VI [8] as well as of RhoA, Rac1, Rho-dependent-kinase and PAK kinase [9–11]. Only two actin-binding proteins have been cloned and sequenced so far, and these are: conventional myosin heavy chain [12] and amebin (formerly termed as ApABP-FI; [13]).

Amebin is a 95-kDa (migrating in the SDS–PAGE gel as 120-kDa protein band) actin-binding protein with N-terminal calponin homology domain followed by only one filamin repeat, a central

* Corresponding author. Address: Nencki Institute of Experimental Biology, Department of Biochemistry, 3 Pasteur St., 02-093 Warsaw, Poland. Fax: +48 22 8225342.
E-mail address: j.redowicz@nencki.gov.pl (M.J. Rędowicz).

0003-9861/$ - see front matter © 2010 Elsevier Inc. All rights reserved.
doi:10.1016/j.abb.2010.11.013

α-helical region exhibiting large probability of coiled-coil formation, and C-terminal region without significant similarity to any known domain/protein (GenBank Accession No. DQ374440, [13]). The domain pattern excludes the possibility that amebin is an orthologue of gelation factors (ABP120) expressed in pathogenic *Enthamoeba histolytica* and slime mold *Dictyostelium discoideum*, because these proteins contain two calponin domains, and four and six filamin repeats, respectively [14,15]. C-amebin, a product of a short 1125-nt transcript constituting 3′ region of amebin 2672-nt cDNA, is composed of 375 amino-acid residues. With the use of a custom made antibody directed against C-terminus of amebin, we previously showed that the protein localized to amoeba actin-rich areas, cortex and perinuclear region [13]. Similar localization was observed for *A. proteus* caldesmon immunoanalog [5] as well as Rac1 and PAK immunoanalogs [9,11].

Here, we presented biochemical characterization of recombinant C-amebin, the first ever recombinant protein based on *A. proteus* cDNA. We showed C-amebin bound to G- and F-actin in Ca^{2+}-independent manner, bundled actin filaments and inhibited actin-activated MgATPase activity of myosin subfragment S1. Also, our data indicate that C-terminus of amebin is involved in interactions with actin. Moreover, blocking endogenous amebin with the specific antibody blocked amoeba motility. These results indicate that amebin may function *in vivo* as one of key regulators of actin dynamics in *A. proteus*.

Materials and methods

Cell culture

Amoeba proteus (strain Princeton) was cultured at room temperature in the standard Pringsheim medium ($Ca(NO_3)_2{\cdot}4H_2O$ – 200 mg/l, $MgSO_4{\cdot}7H_2O$ – 20 mg/l, $Na_2HPO_4{\cdot}2H_2O$ – 20 mg/l, KCl – 26 mg/l, $FeSO_4{\cdot}7H_2O$ – 2 mg/l, pH 6.8–7.2). Amoebae were fed on *Tetrahymena pyriformis* twice a week and always used for experiments on third day after feeding. *Escherichia coli* strain BL21 (DE3) was cultured in Luria Bertani (LB) medium in the presence or absence of 0.5 mM isopropylthio β-D-galactopyranoside (IPTG) for 3 h at 25 °C.

Preparation of Amoeba proteus cytosolic fraction

Amoebae were collected by centrifugation at 2000*g*, washed three times with the ice cold TBS buffer (Tris buffer saline: 150 mM NaCl, 25 mM Tris pH 7.5), homogenized at 4 °C in three volumes of a homogenization buffer containing 10 mM KCl, 2 mM $MgSO_4$, 10 mM imidazole pH 7.0, 1 mM EGTA, 5 mM ATP, 1 mM DTT, 1 mM PMSF, 12% sucrose, and a set of protein inhibitors (“Complete” tablets, Roche). After centrifugation at 100,000*g* for 1 h, the high-speed supernatant (HSS) was taken for further studies.

Protein purification

Recombinant GST-C-amebin fusion protein was expressed in the standard *E. coli* expression system using pGEX-4T2 vector (Amersham Pharmacia, USA). The expressed protein was purified to homogeneity using glutathione-Sepharose 4B beads (Amersham Pharmacia, USA) and used for experiments after an overnight dialysis at 4 °C against 50 mM NaCl, 10 mM HEPES, 0.5 mM PMSF and a set of protein inhibitors (“Complete” tablets from Roche) up to seven days after purification. To obtain a preparation lacking C-terminal region, GST-C-amebin after an exhaustive dialysis against the buffer without protease inhibitors was incubated for 1 h at 25 °C with endoproteinase ArgC (Sigma Aldrich, USA) with the enzyme to protein ratio of about 0.05 units per mg. The preparations were ultracentrifuged for 20 min at 100,000*g* before the experiments. Molecular masses of the polypeptide chains of GST-C-amebin, GST-C-amebin-ArgC and *Schistosoma japonica* GST were taken as 75, 66 and 26 kDa, respectively.

Actin was purified from rabbit skeletal muscle by the standard method of Pardee and Spudich [16] and before use was passed through Sephacryl S-200 column. G-actin was stored in 2 mM Hepes, pH 7.6, 0.1 mM $CaCl_2$, 0.2 mM ATP, 0.02% sodium azide. To obtain filaments, G-actin was polymerized with KCl and $MgCl_2$ up to 100 and 2 mM final concentrations, respectively. Myosin subfragment 1 was obtained from rabbit skeletal muscle as described by Weeds and Pope [17]. Purity of the obtained protein preparations was controlled in 10%, 12% or 15% SDS polyacrylamide gel slabs. For polymerization studies, G-actin was subjected to labeling with *N*-(1pyrenyl)iodoacetamide at cysteine residue 374 as described by [18]. Before use the labelled actin was passed through Sephacryl S-200 column. The yields of labelling was determined spectrophotometrically using pyrenyl absorption coefficient of $2.2 \times 10^4\ M^{-1}\ cm^{-1}$ at 344 nm and were found to be about 70–90%.

Actin-binding studies

To test binding of GST-C-amebin (intact or lacking C-terminal region) to actin filaments, the protein was incubated with 20 μM rabbit skeletal muscle F-actin in the presence of 0.1 mM $CaCl_2$ or 0.2 mM EGTA for 60 min at 4 °C. This was followed by 1-h ultracentrifugation at 150,000*g*. The amount of GST-amebin in the pellet and supernatant fractions was quantified by densitometric analysis of the Coomassie-stained SDS gels using G:Box system from SynGene (Cambridge, UK) equipped with Gene Snap and GeneTools software. Control experiments were performed with GST alone.

To test whether native amebin and C-amebin bind to actin, *Amoeba proteus* high speed supernatants (HSS) were dialyzed overnight at 4 °C against 5 mM $MgCl_2$, 10 mM NaCl, 10 mM Hepes buffer pH 7.5, 1 mM DTT, 1 mM PMSF, and a set of protein inhibitors (“Complete” tablets) and then subjected to the actin-affinity chromatography, based in the principle on the method developed by Miller and Alberts [19]. Carboxy-terminated magnetic particles (Sigma, USA) were activated by extensive washes in a coupling buffer (0.01 M potassium phosphate containing 0.15 M NaCl, pH 5.5), and bound to about 20 μM rabbit skeletal muscle G-actin using EDC (*N*-(3-dimethylaminopropyl)-*N*′-ethylcarbodiimide) as a coupling agent. Though actin was added in the monomeric form it is certain that under these salt conditions it polymerized into filaments that coupled to the beads. The coupling reaction was performed overnight at 4 °C while maintaining the pH between 4.5 and 6.0 with 0.1 M HCl and gentle shaking. Coupling was terminated by dilution with a wash buffer containing 0.01 M Tris, 0.15 M NaCl, 0.1% (w/v) bovine serum albumin, 1 mM EDTA, 0.1% NaN_3, pH 7.4. The actin-bound beads were then extensively washed in the dialysis buffer. After a complete removal of any unattached actin (tested by measuring OD at 280 nm and gel electrophoresis), the beads were combined with the dialyzed HSS (at 1:1 v/v ratio), and the mixture was incubated overnight at 4 °C with a gentle rocking. The actin-affinity beads were then extensively washed, and the bound proteins were eluted using the standard electrophoresis SDS-sample buffer. The presence of amebin and C-amebin in the eluate was tested by mass spectrometry analysis.

Polymerization studies

Effect of GST-C-amebin on actin polymerization was monitored at 25 °C as the increase either in the intensity of pyrene-actin fluorescence at 407 nm after excitation at 365 nm or in the

intensity of light scattering at 400 nm. Spex Fluorolog 3 spectrofluorimeter (Spex Industries, Edison, NJ, USA) was used. Also, light scattering measurements were applied for testing the effect of GST-C-amebin on actin filament bundling.

The experiments were performed in the absence and presence of GST-C-amebin or GST that were added to 4 μM actin in molar ratios to actin of 1:2, 1:4, 1:5 or 1:10, as indicated in the legends to Figs. 6 and 7. Total volume of the reaction mixture was 1 ml. Polymerization was initiated by adding of $MgCl_2$ and KCl to 2 and 100 mM final concentrations, respectively.

Mass spectrometry analysis

Bands corresponding to ~120-kDa and ~60 kDa proteins of the actin-affinity eluate (see Section "Actin-binding studies"), or GST-C-amebin and GST-C-amebin-ArgC were excised from the SDS–PAGE 10% gel and subjected to a mass spectroscopic analysis. After elution of the protein from the gel using an acetonitrile-ammonium bicarbonate-based procedure followed by the standard tryptic digestion, the samples were run on Micromass Q-Tof instrument upgraded to 10,000 resolution, equipped with nano HPLC (LC packings) and matrix assisted laser desorption ionization (MALDI) instrument (MCLDI R). The attained peptide sequences were compared with the sequence of amebin (GenBank Accession No. DQ374440).

Dissociation constant of the GST-C-amebin/actin complex

Dissociation constant K_d was determined in the co-sedimentation experiments performed substantially as described in Section "Actin-binding studies". In these experiments, F-actin (8 μM) was incubated with increasing concentrations of GST-C-amebin (from 1 to 8 μM final concentration). For control experiments, sedimentation of GST-C-amebin without actin was performed and results were included into the calculation. The obtained data were fitted to the binding equation:

$$\text{GST-C-amebin}_{bound} = [\text{F-actin}] * [\text{GST-C-amebin}_{free}]/(K_d + [\text{GST-C-amebin}_{free}])$$

where [F-actin] represents the concentration of filamentous actin and [GST-C-amebin] – the concentration of GST-C-amebin. The presumption was that the binding between actin and GST-C-amebin polypeptide chain was 1:1 (mole:mole).

Cross-linking

To check whether GST-C-amebin binds directly to G-actin and myosin heads, 5 μM protein (intact or lacking the C-terminus) was incubated with 20 mM *N*-ethyl-*N*′-(3-dimethylaminopropyl)carbodiimide (EDC, Sigma, USA) and 5 mM *N*-hydroxysuccinimide (NHS, Sigma, USA) in the presence or absence of 20 μM monomeric actin or 2 μM S1. The mixtures were incubated on ice (or at room temperature for presenting dimer formation of GST-C-amebin) for 60 min, and the reactions were stopped with the Laemmli sample buffer. Control experiments were performed with GST, actin or S1 preparations. Proteins were separated using 8% or 12% SDS–polyacrylamide gels.

Transmission electron microscopy (TEM)

F-actin (4 μM) was mixed with the increasing concentrations (from 0.4 to 2 μM) of GST-C-amebin (intact or lacking C-terminus) in a buffer containing 50 mM NaCl, 0.5 mM PMSF, 10 mM HEPES, pH 7.6. After incubation for 1 h at 25 °C, 10-μl aliquots were applied to carbon coated copper grids (400 mesh/inch) for 40 s and negatively stained (for 25 s) with 2% aqueous uranyl acetate. Grids were blotted and left to dry at room temperature, and then examined using a JEOL JEM-12000 EX electron microscope at an accelerating voltage of 80 kV. GST-C-amebin was visualized with JEOL JEM 1400 electron microscope equipped with a high resolution digital camera (CCD, Morada).

FPLC chromatography

GST-C-amebin and GST (2 mg/ml) in 10 mM HEPES, 50 mM NaCl, 0.5 mM PMSF and 1 mM DTT were subjected to gel filtration at 4 °C at a flow rate of 0.5 ml/min on a Superdex-200 (Amersham Biosciences) column pre-equilibrated in the above buffer. Protein elution was monitored at 280 nm. Cytochrome C (12.4 kDa, elution at 34 min), carbonic anhydrase (29 kDa, 33 min), bovine serum albumin (66 kDa, 29 min), alcohol dehydrogenase (150 kDa, 27 min), β-amylase (200 kDa, 24 min) and dextran (2000, 16 min) were used as molecular mass markers.

Immunoblotting

Amoeba proteus homogenate or GST-C-amebin and its degradation product were separated using 10% and 12% polyacrylamide gels, respectively, and then transferred to a nitrocellulose membrane. After transfer, the membrane was blocked for 1 h at room temperature in TBS containing 5% non-fat milk powder, 0.2% Triton X-100 followed by 1-h incubation with 1:1000 dilution of polyclonal antibodies directed against GST (Affinity Bioreagents, USA), and C-terminus of amebin (produced by EZBiolab, details see in [13]), and when needed monoclonal antibody against *Amoeba proteus* actin (Sigma, USA). Primary antibodies were detected using 1:10,000 dilutions of anti-rabbit antibodies conjugated with horse radish peroxidase and the reaction was developed using the ECL method (Pierce, USA).

ATPase activity measurements

To test the effects of GST-amebin on the actin-dependent MgATPase activity of rabbit skeletal myosin subfragment 1 (S1), measurements were performed in a buffer containing 50 mM NaCl, 10 mM HEPES pH 7.6 and 0.5 mM PMSF and implemented with 2 mM $MgCl_2$ in the presence of 10 μM rabbit skeletal F-actin, 2 μM S1, and 1 or 2 μM GST-amebin or its fragment lacking C-terminus. Samples were incubated for 5 min at 25 °C, and the reaction was initiated by the addition of ATP up to 2 mM final concentration and terminated after 1 min with 2.5% SDS (final concentration). The amount of the released inorganic phosphate was calculated according to the calorimetric Fiske-SubbaRow method [20]. Control experiments were done in the presence of GST alone.

Circular dichroism

To characterize the secondary structure of GST-C-amebin, circular dichroism measurements were performed on a Jasco-810 spectropolarimeter using a 1-mm-path-length cuvette. The concentration of GST-C-amebin was 1.9 mg/ml. Spectra were measured in 0.1 M sodium phosphate buffer pH 7.4 at 25 °C and corrected by substraction of a buffer spectrum. Scans were recorded from 190 to 260 nm, in 1-nm intervals. Data demonstrate the representative experiment out of three performed. GST (2 mg/ml) measurements were performed as the control. The insert represents the difference between GST-C-amebin and GST spectra.

Microinjection

Effect of blocking the endogenous amebin on amoebae behavior was assessed by observing the cells microinjected with the specific antibody raised against C-terminus of amebin (protein concentration of 0.1 mg/ml). Microinjections were carried out directly on standard microscopic slides with glass micropipettes held in an Eppendorf micromanipulator. No additional pipette was needed to hold amoebae still as they were sufficiently strongly attached to the glass surface. Control cells were microinjected with rabbit non-immune serum (protein concentration of 0.1 mg/ml) or with anti-amebin antibody incubated with the peptide against the antibody had been raised. After each microinjection the sequence of up to 400 DIC Nomarski images were over about 60 min acquired using a Nikon inverted microscope equipped with 40 × DIC 0.55NA objective. The images were taken with cooled CCD camera Retiga 1300 (QImaging Co., Canada) connected by firewire interface to PC computer with AQM advance 6 software (Kinetic Imaging Ltd.). Multiple frames were tiled with Photoshop CS9 software (Adobe Inc., USA).

Results

Native amebin binds to actin

Antibody against C-terminus of amebin detected two bands in amoeba homogenates with molecular weights of ~120 kDa and ~60 kDa, confirming that both long (2672-nt) and short (1125-nt) transcripts encoding amebin and C-amebin were expressed in amoebae (Fig. 1A). The lower mobility of the proteins was due to their acidic pI values (5.1 and 4.9 for amebin and C-amebin, respectively) and possibly by its putative elongated shape of both proteins [13]. The immunoreactivity of the antibody with C-amebin was more intensive, which might indicate that either more C-amebin (or other degradation product of amebin with a similar molecular weight) was present in the homogenate and/or the epitope located at C-terminus was more accessible for the antibody. Noteworthy, levels of detection of both proteins (an in particular that of C-amebin) were not much different from the detection level of *Amoeba proteus* actin, using a specific anti-amoeba actin antibody and probing the same sample of homogenate (Fig. 1A).

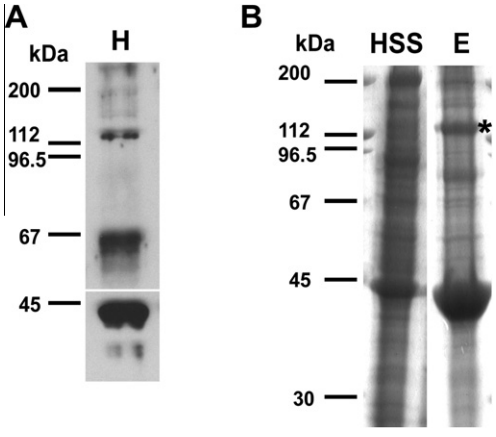

Fig. 1. Native amebin and C-amebin are present in amoebae. (A) Detection of amebin, C-amebin and actin in *Amoeba proteus* homogenate (H). Western blot analysis of the homogenate using the antibodies against C-terminus of amebin (upper part) and amoeba actin (lower part) was performed as described in Section "Immunoblotting". (B) Analysis of the eluate (E) of the actin-bound beads, actin-affinity chromatography of amoebae cytosolic fraction. Amebin (~120 kDa), marked with asterisk, is found in the eluate by means of mass spectrometry. HSS, Coomassie brilliant blue-stained polyacrylamide gel of high-speed supernatant. The experiment was performed as described in Section "Actin-binding studies".

Also, amebin was found among the proteins eluted from the actin-bound beads and was one of most abundant proteins (Fig. 1B, asterisk).

Characterization of GST-C-amebin

To characterize the actin-binding properties of C-amebin (and indirectly of amebin), a recombinant GST-C-amebin fusion protein was produced.

To verify the identity of the recombinant protein, Western blot technique was applied with the use of the antibodies directed against GST and C-terminus of amebin (Fig. 2A and B). Theoretical molecular weight of the C-amebin peptide chain is ~40 kDa and of GST-C-amebin – ~66 kDa. The GST-C-amebin fusion protein migrated, however, as a 75-kDa protein (Fig. 2A), which was most probably due to its low pI (4,9) value and elongated shape of the amebin moiety. Both antibodies recognized the 75-kDa protein, confirming the identity of GST-C-amebin. An attempt was made to remove the GST moiety, but limited proteolysis with several proteases (including thrombin, trypsin, chymotrypsin, V8 protease and factor Xa) did not yield any stable digestion product (not shown). Only cleavage with endoproteinase ArgC resulted in formation of a stable 66-kDa fragment (termed as GST-C-amebin-ArgC) lacking the C-terminus, as it was not detected with the antibody against C-terminus of amebin (Fig 2B). It is difficult to assess the precise cleavage site within amebin C-terminal portion because there are several potential arginine residues susceptible for this protease (Fig. 2C). However, based on a size of the removed fragment (~9 kDa) it is plausible that the cleavage took place at the arginine residues 303, 313 and/or 329. Unfortunately, mass spectrometry analysis was not helpful in determining the cleavage site.

Bioinformatic analysis had revealed that C-terminal region of amebin did not show significant homology to any known protein and predicted high content of α-helical structures as well as regions of low complexity [13]. Indeed, analysis of circular dichroism spectra showed that α-helix was a predominant component of the C-amebin moiety of the fusion protein (Fig. 3A and insert).

Gel filtration revealed that GST-C-amebin was eluted in a fraction corresponding to a protein of molecular weight higher than 200 kDa, which was different than 75 kDa observed on SDS-gel electrophoresis (Fig. 3B). This discrepancy might be due to the elongated shape of the C-amebin and/or its ability to form dimers (or more complex oligomers). However, the presence of the smaller peak between 17 and 20 min of the column run indicate that GST-C-amebin may have tendency to aggregate.

To check whether GST-C-amebin may form dimers, cross-linking studies were performed. As seen in Fig. 3C, in the sample subjected to EDC-NHS crosslinking (see Section "Cross-linking") at room temperature a band corresponding to a protein with molecular weight of about 200 kDa was detected with the anti-amebin antibody. Noteworthy, similar molecular weight was seen for a main gel filtration peak containing GST-C-amebin. Formation of dimers was also noticeable for GST alone and GST-C-amebin lacking C-terminus (not shown), indicating that the GST-moiety (known to form dimers; [21]) and not C-terminus of amebin, is engaged in the observed dimerization.

Noteworthy, we showed earlier that also endogenous amebin seems to form dimers, most probably through its putative coiled-coil domain in the middle of its polypeptide chain [13], thus GST-C-amebin dimer may resemble to some extent the *in vivo* dimers of amebin.

Actin binding

Herein and in our earlier work [13], we demonstrated that native amebin (present in *A. proteus* cellular fractions) bound to

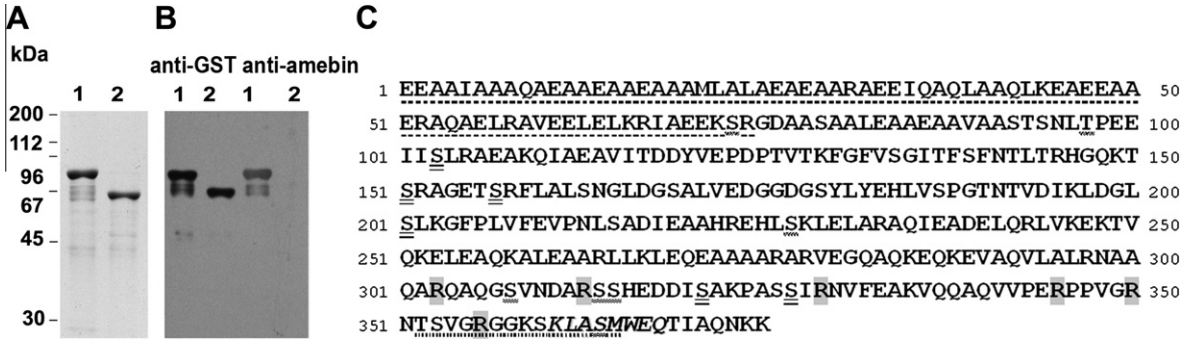

Fig. 2. Confirmation of identity of GST-C-amebin. (A) Coomassie brilliant blue-stained polyacrylamide gel; (B) Western blot using the antibodies against GST and C-terminus of amebin. GST-C-amebin (1) and GST-C-amebin-ArgC (2) interacted with anti-GST antibody but only GST-C-amebin interacted with antibody against C-terminus of amebin. Further details are described in Sections "Protein purification" and "Immunoblotting". (C) Amino-acid sequence of C-amebin. Underlined sequence – α-helical region; S – casein kinase II putative phosphorylation sites; S – protein kinase C putative phosphorylation sites; dotted-underlined letters – sequence of a peptide against which the anti-amebin antibody was raised; italic font – a putative actin-binding sequence; R – putative endoproteinase ArgC cleavage sites.

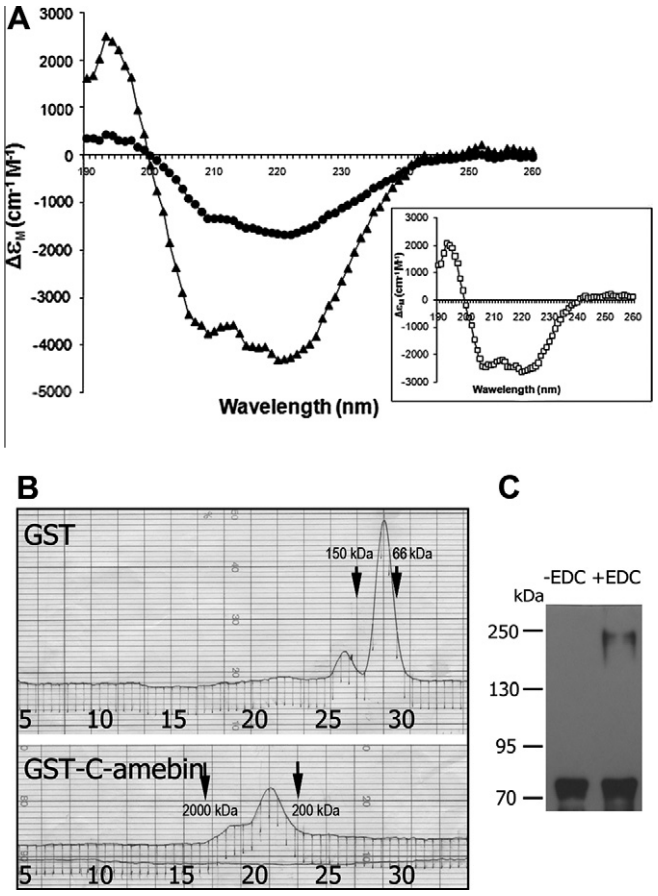

Fig. 3. Characterization of GST-C-amebin structure. (A) CD measurements of GST-C-amebin (▲) and GST (●). An insert, a difference between spectra of GST-C-amebin and GST; further details in Section "Circular dichroism". (B) Elution profiles of GST-C-amebin and GST. Numbers under the elution profiles reflect time (in minutes) after initiation of separation. Arrows point to the elution of the marker proteins; further details in Section "FPLC chromatography". (C) Cross-linking of GST-C-amebin; further details at Section "Cross-linking".

rabbit skeletal F-actin. The assumption was that its calponin-homology domain was involved in the binding. C-terminus of amebin is highly positively charged and resembles to some extent the actin-binding and inhibitory site 2 of caldesmon. However, there was no C-amebin among the actin-bound proteins of amoeba cytosolic fraction, indicating that either it did not bound to skeletal muscle actin or the binding was weak (no calponin-homology domain) and under the experimental conditions used here it could not be observed. Also, there is a possibility that C-amebin was not detected due to mass spectrometry limitations.

We attempted to test whether GST-C-amebin, lacking the calponin homology domain and filamin repeat but containing a potential actin-binding site, could interact with actin. The cross-linking with a zero-length crosslinker (EDC) as well as sedimentation assays were performed (Figs. 4 and 5).

When GST-amebin was incubated with G-actin in the presence of EDC at 0 °C, a cross-linking product with a molecular weight of ~112 kDa was formed, corresponding to the approximate sum of molecular weights of GST-C-amebin and monomeric actin (Fig. 4). No visible cross-linking product was formed when GST alone was incubated with EDC in the presence of actin, thus indicating that C-amebin but not GST was involved in the binding. Interestingly, no cross-linking product was formed when GST-C-amebin-ArgC was incubated with actin monomers, implying that a positively charged C-terminal region of amebin might comprise additional actin-binding site.

Similar conclusions were obtained in the course of actin-sedimentation assays (Fig. 5). When GST-amebin was incubated with rabbit skeletal F-actin and then ultracentrifuged, the vast majority of the protein sedimented into a pellet together with actin filaments (Fig. 5A). The binding was independent on calcium ions as the same data were obtained in the presence or absence of $CaCl_2$

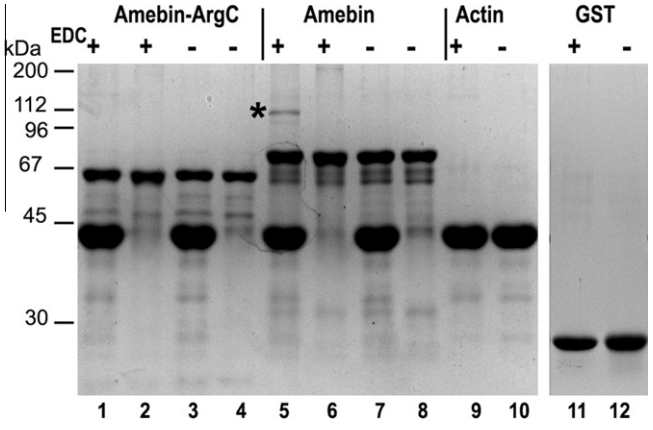

Fig. 4. C-amebin binds to monomeric actin. GST-C-amebin (lanes 5–8) and GST-C-amebin ArgC (lanes 1–4) were incubated with G-actin (lanes 1,3,5 and 7) in the presence (lanes 1, 2, 5 and 6) or absence (3, 4, 7 and 8) of EDC. G-actin (lanes 9 and 10) and GST (11 and 12) and were used as the controls. A 112-kDa cross-linking product has been marked with an asterisk (lane 5). Further details are described in Section "Cross-linking".

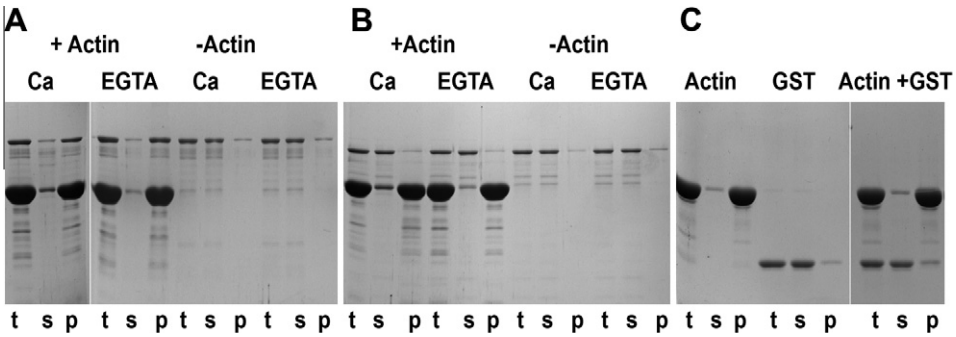

Fig. 5. C-amebin binds to filamentous actin in Ca^{2+}-independent manner. GST-amebin (A) and GST-amebin-ArgC (B) were incubated with filamentous actin in the presence or absence of Ca^{2+}, as indicated. The samples were next ultracentrifuged, and the presence of proteins in the total (t) as well as in the supernatant (s) and pellet fractions (p) was analyzed. As the controls (C), the GST and actin alone, as well as the actin and GST mixture were treated analogously to the tested samples. Further details are described in Section "Actin-binding studies".

(Fig. 4A). Also, neither GST (Fig. 5C) nor GST-C-amebin-ArgC was seen in the pellets (Fig. 5B).

The actin sedimentation assay performed in the increasing concentrations of GST-C-amebin (from 1 to 8 μM) yielded the dissociation constant (K_d) of $\sim 1.2 \times 10^6\ M^{-1}$. The calculations were made based on the data from four independent experiments with the assumption of GST-C-amebin polypeptide chain binds to actin monomer in the molar ratio of 1:1.

Effect of GST-C-amebin on actin polymerization

In order to test whether binding of GST-C-amebin to G-actin promotes filament formation, the course of actin polymerization was monitored in the presence of GST-C-amebin and, as a control, in the presence of GST alone. Light scattering technique and fluorescent method, monitoring changes of fluorescence intensity of pyrenyl label non-covalently attached to cysteine 374 residue of actin, were applied (Fig. 6A and B). Polymerization was initiated by adding 2 mM $MgCl_2$ and 100 mM KCl. GST or GST-C-amebin were added about 20 s before addition of polymerizing solution. No effect of GST-amebin and GST on G-actin samples was observed without addition of 2 mM $MgCl_2$/100 mM KCl (not shown).

As shown in Fig. 6A and B (lines 1 and 2), the curves corresponding to polymerization of actin alone and in the presence of GST (in 1:5 GST to actin molar ratio as an example) were practically identical, indicating that GST did not affect the polymerization process. Contrary to that, GST-C-amebin significantly affected the polymerization course. However, the effects were dependent on a method used for monitoring the polymerization process. When the fluorescent method was applied, the addition of GST-C-amebin caused decrease of the pyrenyl fluorescence and the observed decrease was dependent on the amount of the added protein (Fig. 6A), with the lowest fluorescence values for GST-C-amebin added in 1:2 M ratio to actin. Contrary to that, light scattering measurements showed that immediately after adding $MgCl_2$/KCl, the signal intensity increased in comparison with the one observed for actin alone (Fig. 6B). The highest increase during first minutes of the experiment was observed for the mixture of 1:2 amebin to actin (Fig. 6B, arrow).

Close inspection of the mixture-cointaining cuvettes 1 h after salt addition revealed the presence of either opalescence across the entire sample (ratios of amebin to actin of 1:4, 1:5 or 1:10) or a clumpy precipitate floating in the cuvette (ratio 1:2), indicating formation of more complex actin structures but not actin filaments. Therefore, this is most probably the reason of the observed decay of pyrenyl fluorescence upon adding of increasing amounts of GST-C-amebin.

To confirm whether GST-C-amebin stimulated formation of more complex actin filament structures, GST-C-amebin and F-actin mixtures were subjected to light scattering measurements. Representative results out of several experiments, in which GST-C-amebin was added in the 1:2 M ratio, are presented in Fig. 7. As seen, about an order of magnitude increase in the light scattering was observed, indicating formation either of actin bundles or a dense actin network. Similarly to the actin polymerization studies, a clumpy precipitate was formed and was floating in the cuvette, causing fluctuation of the light scattering.

Analogously to actin polymerization studies, GST alone did not affect the light scattering measurements.

Electron microscopy studies of GST-C-amebin and actin complexes

In order to visualize actin structures formed in the absence or presence of GST-C-amebin, transmission electron microscopy was applied (Fig. 8). Micrographs of GST-C-amebin alone were also presented (Fig. 8D). The samples for the analysis were taken at the end of the polymerization experiments described in Section "Effect of GST-C-ambein on actin polymerization", approximately one hour after adding GST-C-amebin to F-actin.

GST-C-amebin added to filamentous actin (Fig. 8A, E–G) in all ratios studied (1:10, 1:5 and 1:2) caused formation of long actin bundles. Size of the bundles varied, reaching the length of tens of micrometers and width from 50 nm to almost 1 micrometer. Also, micrographs show that bundles formed in the presence of the highest GST-C-amebin concentration (Fig. 8G) seem to be the most electron dense, indicating that they might be more packed. This could explain the formation of the clumpy precipitate formed when C-amebin was added in the ratio of 1:2.

GST-C-amebin alone formed V-shaped structures (Fig. 8D) with the length of the arms varying from 20–30 nm. However, GST-C-amebin tetramers or more oligomerized structures could be also visible. Neither GST (Fig. 8B) nor GST-C-amebin lacking C-terminal fragment (GST-amebin-ArgC; Fig. 8C) stimulated bundle formation, indicating again that the positively charged C-terminal fragment of the amebin moiety could be involved in the observed interactions with both monomeric and filamentous actin.

Effect of GST-C-amebin on actin-activated ATPase activity of myosin subfragment 1

Since C-amebin interacted with actin it was obvious to check whether it might affect actin-activated myosin MgATPase activity. The experiments were performed using rabbit skeletal muscle actin and myosin subfragment 1 (S1; Fig. 9A). When acto-S1 ATPase activity was measured in the presence of GST-C-amebin in molar ratios to actin of 1:10 and 1:5 (i.e., 1 and 2 μM, columns 6 and 7), significant decrease of the activity was observed as compared to the acto-S1 activity (column 5). The decrease was by about

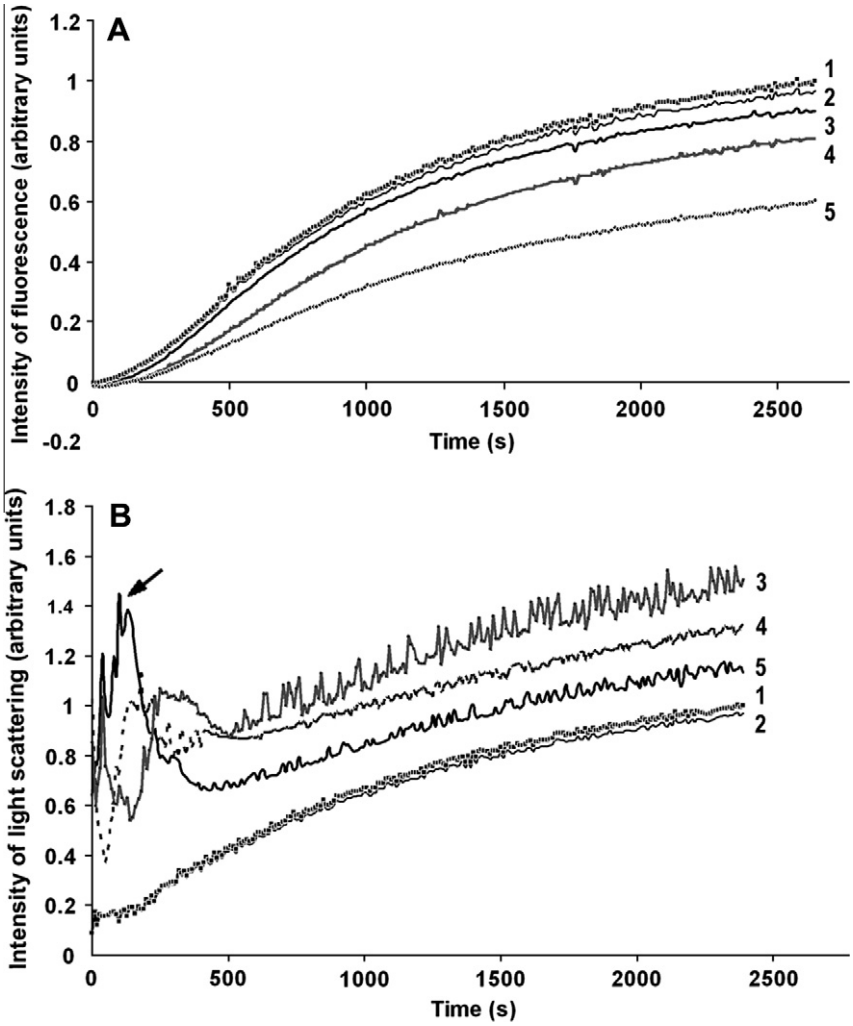

Fig. 6. Amebin but not GST affects actin polymerization. Effect of GST-C-amebin on salt-induced polymerization of G-actin was monitored by changes in (A) fluorescence of pyrenyl non-covalently attached to cysteine 374 residue of actin and (B) light scattering. Fluorescence measurements were performed in the presence of GST-C-amebin at molar ratios to actin of 1:2 (line 5), 1:5 (line 4) and 1:10 (line 3); and light scattering was measured at the ratios of 1:2 (line 5), 1:4 (line 4) and 1:5 (line 3). Measurements in the presence of GST were performed at the ratio of 1:5 (line 2 in both plots); lines 1 represent polymerization of actin alone. Further details are described in Section "Polymerization studies".

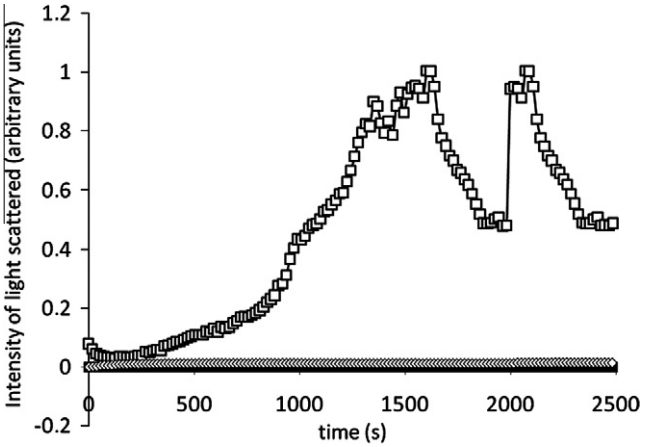

Fig. 7. C-amebin added to F-actin at the molar ratio of 1:2 (□) caused a significant increase of light scattering. GST (—) did not affect the signal and resembled that of F-actin-alone (◇). Further details are described in Section "Polymerization studies".

32% and 46% for 1 and 2 μM GST-C-amebin, respectively. Inhibition was not observed for GST (lanes 12 and 13) or the GST-C-amebin fragment lacking C-terminus (columns 8 and 9), implying that C-terminus of amebin moiety was responsible for the observed decrease of the acto-S1 MgATPase activity. Due to technical reasons (formation of the precipitate), activity could not be measured at the ratio of 1:2 of GST-C-amebin to actin.

In order to reveal whether the observed inhibition resulted solely from the interaction of amebin with actin, the EDC-cross-linking of GST-amebin with S1 was preformed. No cross-linking product was formed, indicating that S1 and C-amebin moiety did not interact directly (not shown). It implies that the observed effect of amebin on the acto-S1 ATPase activity might result from the interaction of amebin with actin filaments and not with the myosin head domain. On the other hand, when the ATPase reaction mixture was analyzed by electron microscopy, the dissolution of the bundles was observed (Fig. 9B).

Effect of the antibody against C-terminus of amebin on amoeba migration

To test whether the observed interactions between amebin and actin could be relevant *in vivo*, we first attempted microinjection of amoebae with GST-C-amebin and GST-C-amebin-ArgC. However,

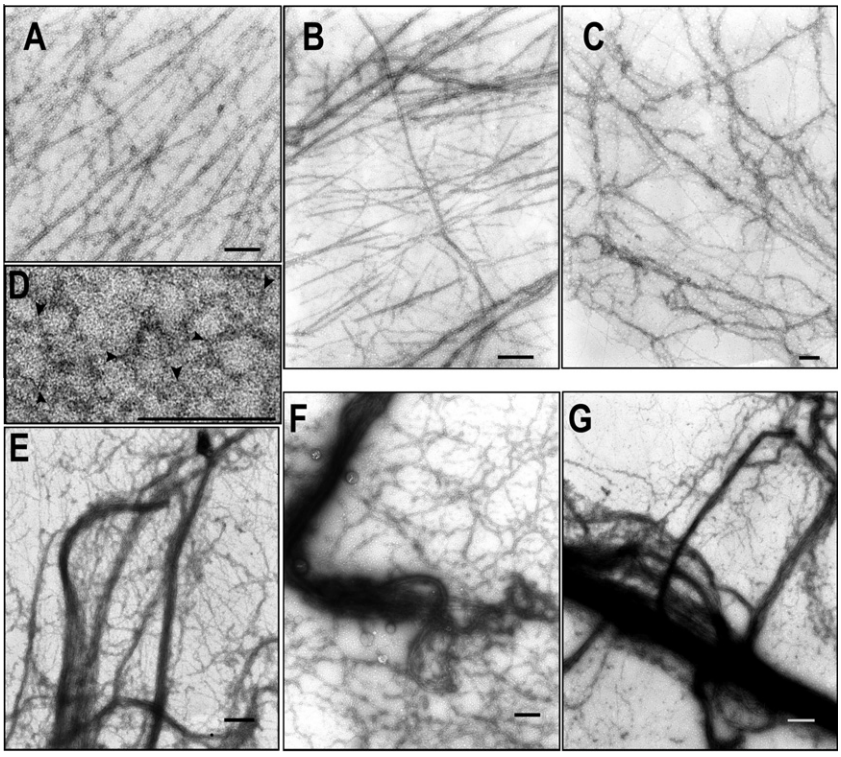

Fig. 8. Actin filament bundles are formed in the presence of GST-C-amebin. Actin filaments (A) were incubated for 60 min in the presence of GST (B); GST-amebin (E–G) or GST-amebin-ArgC (C), the mixtures were applied on the grids and subjected to the transmission electron microscopy analysis. The molar ratios of the added proteins to actin are as follows: B, 1:5; C, 1:5; E, 1:10; F, 1:5; G, 1:2. D, GST-C-amebin; arrowheads point to tips of V-shaped structures. Further details are described in Section "Transmission electron microscopy (TEM)". Bar – 100 nm; Bar: A–B and E–G, 500 nm; C, 200 nm and D, 100 nm.

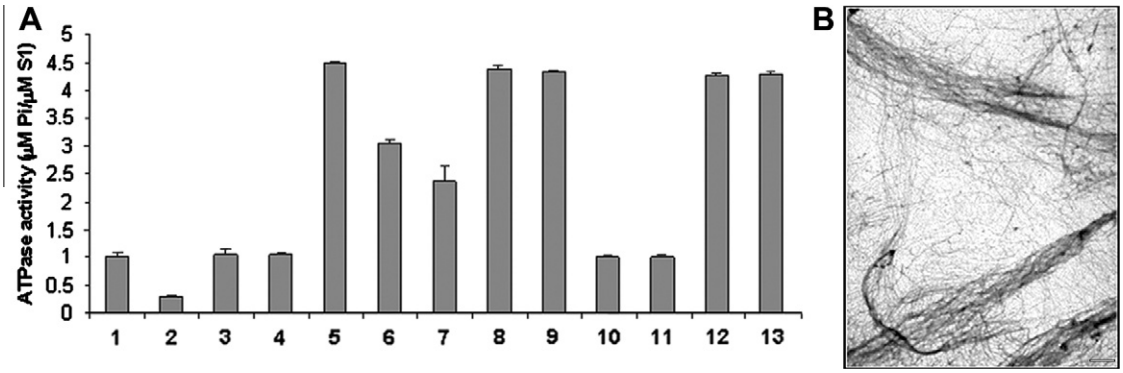

Fig. 9. C-amebin inhibits MgATPase activity of skeletal muscle acto-S1. (A) ATPase measurements were performed as described in Section "Immunoblotting". Bars represent MgTPase activities of: **1**, S1; **2**, F-actin alone; **3** and **4**, S1 in the presence of, respectively, 1 and 2 μM GST-amebin; **5**, acto-S1; **6** and **7**, acto-S1 in the presence of, respectively, 1 and 2 μM GST-C-amebin, **8** and **9**, acto-S1 in the presence of, respectively, 1 and 2 μM GST-C-amebin-ArgC; **10** and **11**, S1 in the presence of, respectively, 1 and 2 μM GST; **12** and **13**, acto-S1 in the presence of, respectively, 1 and 2 μM GST. The presented data are obtained from three independent experiments performed in duplicates. Further details in Section "ATPase activity measurements". (B) Amebin-induced actin bundles dissolve into a network upon addition of S1 and MgATP, in the conditions of the ATPase assay (molar ratio amebin to actin of 1:5). The mixture was applied on the grid and subjected to the transmission electron microscopy analysis. Bar 500 nm.

the observed effects were nearly identical to those caused by GST alone. After introducing GST (as well as both C-amebin preparations) amoebae rounded up, the granules darkened and concentrated at the cell center and within first 5–8 min cell integrity was disrupted, causing cell death most probably due to severe changes in the redox state evoked by GST (not shown).

Therefore, amoebae were microinjected with anti-amebin antibody (see the antigen sequence in Fig. 2C). The results obtained for the treated (Fig. 10A) and control cells (Fig. 10B and C), microinjected with non-immune serum or anti-amebin antibody preincubated with the blocking peptide are presented.

Immediately after injection, amoebae treated with the antibody rounded up into a rossette form and stopped to migrate (Fig. 10A). Also, the movement of cytoplasmic granules was halted. These effects, unlike that for two types control cells, were observed during the course of the experiment that lasted for about one hour. Hence, blocking endogenous amebin severely affected organization of actin cytoskeleton and disturbed cell polarization as well as intracellular translocation and cell locomotion.

Discussion

Our results demonstrate that C-amebin, first *Amoeba proteus* recombinant protein, bound to monomeric and filamentous actin, bundled actin filaments and inhibited MgATPase activity of acto-S1, and the positively charged C-terminal region of the protein could be engaged in these properties. The interaction of amebin (and C-amebin) with actin seemed to be important *in vivo* as

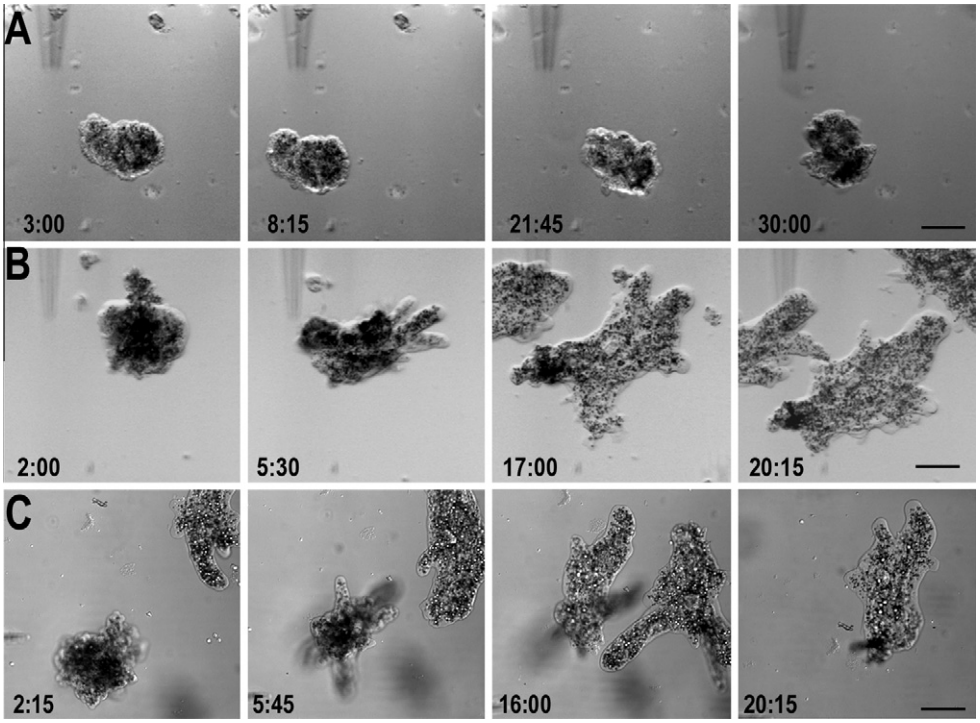

Fig. 10. Effect of blocking endogenous amebin (and C-amebin) on amoeba morphology and migration. Cells were microinjected either with polyclonal antibody directed against C-terminus of amebin (A), with rabbit non-immune serum (B) or with anti-amebin antibody preincubated with the blocking peptide against which the antibody was produced. (C) Numbers in the right bottom corner of each panel reflect time (in min) after the treatment. Further details are described in Section "Microinjection". Bar 100 μm.

introducing into the cell antibody directed against C-terminus of amebin, detecting both proteins, severely affected amoeba motility.

C-amebin consists of a short sequence of the putative coiled-coil domain and C-terminal region of the full length amebin. Both proteins were detected in amoeba homogenates in different levels (see Fig. 1) and not much different (especially C-amebin) from that of actin. However, we are aware that Western blotting is only a semi-quantitative method, dependent mainly on the accessibility of antigen. We showed earlier [13], endogenous amebin colocalized with filamentous actin *in vivo*, and bound to rabbit skeletal actin. Here we showed, analyzing the eluate of the actin-affinity chromatography, that amebin is one of most abundant actin-binding proteins of amoeba cytosolic fraction. We assume that the binding occurs *via* calponin-homology (CH) domain, which *nota bene* is not similar to any CH domain of the known actin binding proteins [13]. It has been reported that proteins containing one CH domain interacted with actin filaments less tightly [22,23].

Using recombinant C-amebin fused with GST, we demonstrated its interaction with both monomeric and filamentous actin. Binding to actin filaments was Ca^{2+}-independent, and dissociation constant was similar to the values reported for several actin-binding proteins, including skeletal muscle tropomyosin [24], avian gizzard and nonmuscle caldesmons [25], and CacyBP/SIP [26], and induced formation of actin filament bundles. Whereas there are quite a few actin bundling proteins, including caldesmon, fascin, α-actinin and formin [2] as well as CacyBP/SIP [26], none of them has been found in *A. proteus*. It is plausible that full length amebin, potentially acting as a dimer, may be also engaged in filament bundling. C-amebin also caused a significant inhibition of MgATPase activity of acto-S1; the effect was due to its interaction with actin since no binding of amebin to S1 was observed. Most of actin bundling and cross-linking proteins inhibit actomyosin ATPase activity as a result of steric blocking of S1 binding sites on actin protomer (see [27]). Using limited proteolysis we removed ~9 kDa positively charged C-terminal region of amebin (pI > 10, independent on the putative cleavage site) and demonstrated that its removal was responsible for the observed effects. Many actin-binding proteins without the typical actin-binding domain(s) interact with the actin acidic N-terminal region and the binding is based on the charge difference [27]. Analysis of the amino-acid sequence of this positively charged segment of amebin revealed, next to several lysine and arginine residues, the presence of KLASMWEQ region resembling to some extent the actin-binding and inhibitory site 2 of caldesmon – KRNLWEKQ (see [28]). Therefore, this segment might be directly involved in interaction with actin. Since GST-C-amebin forms a V-shaped dimer (*via* its GST moiety) it is possible that both C-terminal fragments of the dimer bind to actin monomer of neighboring filaments. This mechanism may be also utilized *in vivo* as the full length amebin is believed to form dimers *via* its putative coiled-coil domain [13]. However, it cannot be excluded that the observed bundling could be also partially due to the observed tendency of GST-C-amebin to aggregate.

Effect of amebin blocking with the antibody directed against its C-terminus indicates that it may be a key player in maintaining actin cytoskeleton dynamics in these giant cells. Noteworthy, similar phenotype was observed when amoebae were microinjected with antibody against myosin II [own observation, not published], the protein known to be crucial for cell migration and other motile processes.

The question arises as of how the binding between actin and C-amebin might be regulated. One of the possible mechanisms could be phosphorylation as there are several potential phosphorylatable serine and threonine residues in C-amebin sequence, which could be targets for protein kinase C or casein kinase II (Fig. 2C). Although nothing is known about these kinases in *A. proteus*, we expect these and/or other specific amebin kinase(s) are expressed in amoebae. Another way of regulation of amebin-actin interaction could be

related to Ca^{2+} but we did not observe any direct effect of this divalent cation on the binding. Also, in amebin sequence there is no a potential Ca^{2+}-binding domain resembling the ones present in other actin-bundling proteins, including α-actinin [29]. On the other hand, binding of endogenous amebin to actin filaments seemed to be Ca^{2+}-dependent, implying indirect interaction of calcium, as it occured in the case of caldesmon – binding Ca^{2+}-calmodulin [13,28]. We tested binding of Ca^{2+}-calmodulin to C-amebin by monitoring the changes in its intrinsic tryptophan fluorescence but did not observe any difference in the fluorescence intensity (not shown). So, if such interaction occurs, the N-terminal but no C-terminal part of amebin is engaged in calmodulin binding. The other indirect mechanism could be *via* other proteins and/or their ligands.

Interestingly, the interaction of amebin with actin filaments resembled, to some extent, that of caldesmon, and in particular its 35-kDa C-terminal fragment [25,28,30,31]. Both proteins not only formed actin bundles, inhibited acto-S1 ATPase activity but also the stoichiometry of their interaction with actin as well as pI values were comparable. Also, blocking of caldesmon with the antibodies disrupted actin filament organization and motile function of several cell lines [28,32]. While there is no similarity between the entire amebin and caldesmon sequences, there is a significant homology (about 40% identity) between the helical region of amebin (a putative coiled-coil domain) and the spacer region of caldesmon as well as the presence of several amino-acid clusters characteristic for caldesmon, which are scattered throughout amebin sequence, including the above mentioned C-terminal KLASMWEQ sequence. Noteworthy, it was reported that a custom made polyclonal antibody against C-terminus of chicken gizzard caldesmon recognized in *A. proteus* cytosolic fraction two protein bands with apparent molecular weights of ∼120 and ∼60 kDa [5], which were comparable to the bands recognized by anti-amebin antibody. While there is no further evidence for similarity between caldesmon and amebin, it is plausible that amebin may serve as the functional relative of caldesmon. On the other hand, it cannot be excluded that in accordance to the cell specific demands, amebin due to the presence of filamin and calponin domains and a relatively long helical region may fulfill the functions of several actin-binding proteins such as calponin, caldesmon, filamin or tropomyosin, as well as gelation factors, present in early eukaryotic organisms such as *Entamoeba* and *Dictyostelium*.

Taking together, our observations indicate that amebin may be one of key regulators of actin-cytoskeleton dynamics in these giant cells.

Acknowledgments

We would like to thank Professor K. Jeon for his gift of *Amoeba proteus* cDNA library that made this project come to life, Ms. E. Purta and Dr. K. Skowronek for help in CD measurements, Mrs. B. Groszynska for amoebae and Dr. P. Pomorski for his help in microinjection studies. Y.R. and R.S. participated in the project during their practice at the Nencki Institute. This work was supported by a statutory grant to the Nencki Institute from the Ministry of Science and Higher Education and the Polish Network for Mechanisms of Cell Motiliy, *Mobilitas.pl*.

References

[1] T.D. Pollard, G.G. Borisy, Cell 112 (2003) 453–465.
[2] S.J. Winder, K.R. Ayscough, J. Cell Sci. 118 (2005) 651–654.
[3] K.W. Jeon, J. Eukaryot. Microbiol. 42 (1995) 1–7.
[4] W. Stockem, W. Kłopocka, Int. Rev. Cytol. 112 (1988) 137–183.
[5] M. Gągola, W. Kłopocka, A. Grębecki, R. Makuch, Protoplasma 222 (2003) 75–83.
[6] E.Y. Choi, K.W. Jeon, Exp. Cell Res. 199 (1992) 174–178.
[7] K. Brix, A. Reinecke, W. Stockem, Eur. J. Cell Biol. 51 (1990) 279–284.
[8] M. Dominik, W. Kłopocka, P. Pomorski, E. Kocik, M.J. Rędowicz, Cell Motil. Cytoskel. 61 (2005) 172–188.
[9] W. Kłopocka, M.J. Rędowicz, Protoplasma 220 (2003) 163–172.
[10] W. Kłopocka, M.J. Rędowicz, Protoplasma 224 (2004) 113–121.
[11] W. Kłopocka, J. Moraczewska, M.J. Rędowicz, Protoplasma 225 (2005) 77–84.
[12] S.W. Oh, K.W. Jeon, J. Eukaryot. Microbiol. 45 (1998) 600–605.
[13] M. Sobczak, E. Kocik, M.J. Rędowicz, Biochem. Cell Biol. 85 (2007) 1–11.
[14] M. Vargas, P. Sansonetti, N. Guillen, Mol. Microbiol. 22 (1996) 849–857.
[15] A.A. Noegel, S. Rapp, F. Lottspeich, M. Schleicher, M. Stewart, J. Cell Biol. 109 (1989) 607–618.
[16] J.D. Pardee, J.A. Spudich, Methods Enzymol. 85 (1982) 164–181.
[17] A.G. Weeds, B. Pope, J. Mol. Biol. 111 (1977) 129–157.
[18] T. Kouyama, K. Mihashi, Eur. J. Biochem. 114 (1981) 33–38.
[19] K.G. Miller, B.M. Alberts, Proc. Natl. Acad. Sci. USA 86 (1989) 4808–4812.
[20] C.H. Fiske, Y. SubbaRow, J. Biol. Chem. 66 (1925) 375–400.
[21] D. Sheehan, T.J. Mantle, Biochem. J. 218 (1984) 893–897.
[22] M. Gimona, K. Djinovic-Carugo, W.J. Kranewitter, S.J. Winder, FEBS Lett. 513 (2002) 98–106.
[23] E. Korenbaum, F. Rivero, J. Cell Sci. 115 (2002) 3543–3545.
[24] A. Wegner, K. Ruhnau, Biochemistry 27 (1988) 6994–7000.
[25] M.-P. Arias, M. Pacaud, Biochemistry 40 (2001) 12974–12982.
[26] G. Schneider, K. Nieznański, J. Jóźwiak, Ł.P. Słomnicki, M.J. Rędowicz, A. Filipek, Tubulin binding protein, CacyBP/SIP, induces actin polymerization and may link actin and tubulin cytoskeletons BBA, Mol. Cell Res. 2010. doi:10.1016/j.bbamcr.2010.07.003.
[27] C.G. dos Remedios, D. Chhabra, M. Kekic, I.V. Dedova, M. Tsubakihara, D.A. Berry, N.J. Nosworthy, Physiol. Rev. 83 (2003) 433–473.
[28] J.J.-C. Lin, Y. Li, R.D. Eppinga, Q. Wang, J.-P. Jin, Int. Rev. Cell Mol. Biol. 274 (2009) 1–68.
[29] A.A. Noegel, W. Witke, M. Schleicher, FEBS Lett. 221 (1987) 391–396.
[30] D. Mornet, M.-C. Harricane, E. Audemard, Biochem. Biophys. Res. Commun. 155 (1988) 808–815.
[31] R. Dabrowska, A. Goch, B. Galazkiewicz, H. Osinska, Biochim. Biophys. Acta 842 (1985) 70–75.
[32] C.L. Wang, Adv. Exp. Med. Biol. 644 (2008) 250–272.